

Tool path effects on wrinkling in metal sheet incremental roll profiling

BEIGZADEH Ali^{1,a*}, SIMONETTO Enrico^{1,b}, GHIOTTI Andrea^{1,c},
BRUSCHI Stefania^{1,d}

¹ Department of Industrial Engineering, University of Padova, Via Venezia 1, 35131, Padova, Italy

^aali.beigzadeh@studenti.unipd.it, ^benrico.simonetto.1@unipd.it, ^candrea.ghiotti@unipd.it, ^dstefania.bruschi@unipd.it

Keywords: Incremental Forming, Flexible Roll Bending, Tool Path

Abstract. The paper introduces an innovative Incremental Forming (IF) machine, termed "FlexRoll Bending," designed for flexible sheet forming on straight components. Unlike traditional processes, this machine employs two working rollers that can move along three directions and rotate, eliminating the need for specific dies. The study focuses on an "on-edge forming strategy" to manufacture non-uniform cross-section sheet metal parts, presenting a cost-effective alternative to conventional methods. The experimental setup utilizes a 0.8 mm DD11 steel sheet, and a novel toolpath theory is introduced for calculating the movement of the forming rollers. Numerical simulations in LS-DYNA software assess the impact of different toolpaths on the final geometry, revealing successful part manufacturing without defects using a linear toolpath and identifying wrinkling in a two-stage toolpath. The results demonstrate the potential of the FlexRoll Bending process for die-less manufacturing of complex geometry sheet metal parts with low forming forces.

Introduction

The rise of Industry 4.0 over the last ten years, along with an increased focus on manufacturing to meet customer needs [1], has highlighted the importance of agile and flexible manufacturing strategies across various sectors. This has become particularly evident in the context of the COVID-19 pandemic [2]. Sheet metal forming processes have commonly found application across a range of industries, including automotive [3], shipbuilding, aerospace industries, shell construction, and power plants, for the fabrication of structural components characterized by enhanced stiffness [4]. However, these procedures usually necessitate specific dies or professional personnel capable of implementing complex duties through manual processes. Dealing with large-sized components poses an extra challenge, as conventional metal forming presses frequently lack the required force or table size for bending operations. recently, there has been an increasing call for small-batch and single-production runs, contributing to reduced profitability in these operations [5]. In response, manufacturers aim to stay competitive by providing more flexibility, better quality, quicker time-to-market, and lower production costs [6].

Roll forming (RF) is a well-known process for the manufacturing of long-profile components with a uniform cross-section for applications in various industries such as the automotive, aircraft, and building industries [7]. In roll forming, the metal strip is fed through consecutive sets of rotating rollers. Each forming roller stand performs an incremental part of the bend, and the flange is therefore incrementally bent to the desired shape and angle.

To eliminate the uniform cross-section limitation in the RF process, Flexible Roll Forming (FRF) process has been introduced. In this process, some of the rollers stay stationary while others can move perpendicular to the feeding direction and rotate along the vertical axis to produce varying width and depth parts [8, 9].



In the profiles manufactured by the FRF process, the main failure mode is flange wrinkling [10]. Wrinkling commonly happens in longitudinal or planar compression situations [9] which commonly occurs in non-uniform cross-section regions.

On the other hand, Incremental Forming (IF) processes are gaining attention as a cost-effective option. Unlike traditional methods, IF doesn't need expensive dies and works well for various part shapes and batch sizes [11]. These processes involve minimal tool-sheet contact, allowing controlled plastic deformation with lower applied forces [12].

Several studies have investigated the application of Incremental Forming (IF) processes for both axis-symmetric and elongated parts. For axis-symmetric parts, metal spinning [13] is considered a promising method for manufacturing large and thick components. The design of the tool path [14] is crucial for ensuring workpiece quality, as the circumferential stress resulting from the reduction of the part's average diameter often leads to wrinkles [15] or other defects. Concerning elongated parts, Voswinckel et al. explored stretch and shrink flanging [16] and evaluated the influence of the tool path on part accuracy [17]. Additional studies have investigated pre-forming flanging procedures for stretch, shrink, and hole-shaped flanges [18]. While many studies have used pin-like tools, others have suggested using a single roller-shaped tool for hemming operations [19], often in conjunction with robotic arms. However, employing this combination to maneuver tools along complex 3D paths [20], despite providing increased flexibility, could face limitations due to the equipment's low stiffness and might not be suitable for thicker workpieces [21].

This paper presents an innovative concept for an Incremental Forming (IF) machine designed specifically for flexible sheet forming operations on straight components, utilizing two working rollers which is called "FlexRoll Bending" process [22, 23]. In this newly introduced IF machine, the mechanics of the metal deformation is similar to RF and FRF, while instead of feeding the stripe and using numerous roller sets, the stripe is restrained, and Roller(s) are able to move along the three directions and rotate in one direction. The strategy of using a pair of simple rollers makes the FlexRoll bending process budget friendly. In the previous research, 90° and 180° bents performed successfully using a pair of rollers. On the other hand, the main purpose of manufacturing of mentioned IF machine is completely die-less manufacturing of complex geometry sheet metal parts with low forming forces. Generation of the toolpath is one of the most important challenges for this IF machine. Controlling the movement of two rollers in three directions increases the complexity of the toolpath needed to generate the final component. Therefore, in the experiments of this research, just one of the forming rollers was used to manufacture the parts.

In this study, a novel approach called "on-edge forming strategy" will be introduced for manufacturing parts non-uniform cross-section part which is more complex compared to previously investigated. The target part has been manufactured by using on edge forming strategy with two different toolpaths on the 0.8 mm DD11 sheet.

DD11 is a hot-rolled steel sheet with very low carbon (<0.12% C) content characterized by its favorable formability properties at ambient temperature, making it widely utilized in cold-forming processes, combined with good weldability. The characteristics of this steel render it well-suited for the subsequent manufacturing of a variety of end products, including stamped, pressed, welded, and drawn parts, as well as tubes, car wheels, agricultural equipment, fasteners, and shelving systems.

Material

The reference material is a 0.8 mm thick DD11 sheet. To evaluate the behavior of the mentioned material, dog bone samples with a gauge length of 65 ± 0.1 mm and width of 12 ± 0.05 mm were cut from the sheet along the three rolling (0 deg), perpendicular (90 deg), and 45 deg directions based on the ISO 6892 standard. MTS 322TM hydraulic dynamometer with a maximum load

capacity of 50 kN and strain rate of 0.1 s^{-1} was employed to perform tensile tests. Fig. 1 displays the results of the tensile test along the mentioned directions for the DD11 hot-rolled sheet. Tensile test results demonstrate an average yield strength of 224 MPa, Ultimate Tensile strength of 439 MPa, and Elongation of 21.4%.

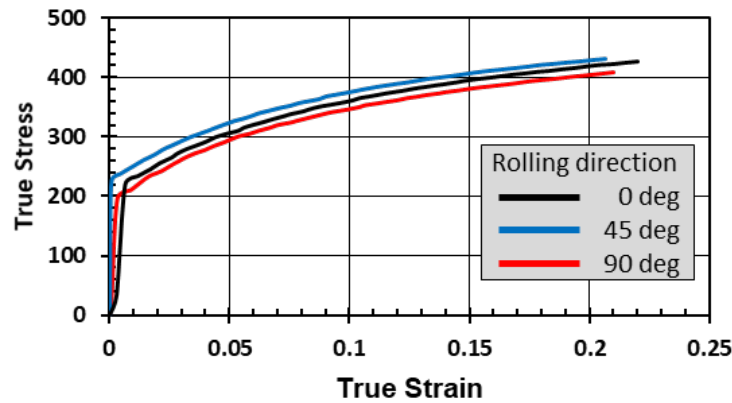


Fig. 1. DD11 flow stress curves along the three directions

Part

The raw material is a 0.8 mm thick DD11 sheet with a length of 500 mm and a width of 150 mm. The sheet metal is bent along the line AA' by movement of the forming roller. In the desired workpiece, the bent angle increases from 0° in BB' section to 60° in CC' section, see Fig. 2. As it illustrated in Fig. 2, $AA'C'B'$ area clamped by the clamping plates.

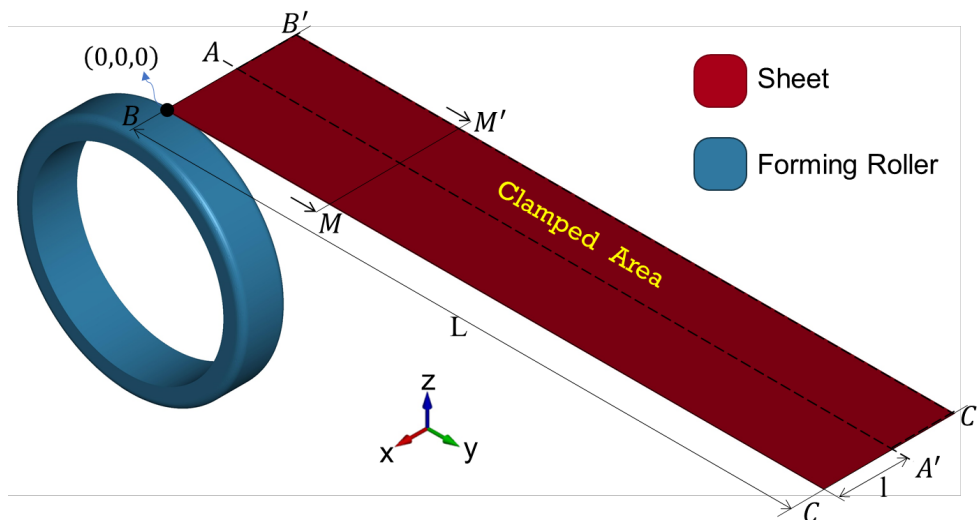


Fig. 2. Schematic of the Flexible Roll Bending process

Toolpath theory

For tool path derivation, the deformation in the FlexRoll bending process must be investigated from the geometrical point of view. In this research, to simplify the process, just one of the rollers was used to form the sheet, and the sheet wasn't supported by the support roller. As an additional simplifying assumption, it has been assumed that the thickness of the sheet doesn't change during the process which is deemed acceptable in consideration of the nature of the deformation applied in this research. As the last simplifying assumption, a perfect bending situation happens. Therefore, the bending allowance area doesn't exist. Therefore, MM' cross-sectional of the Fig. 2 will be like Fig. 3.

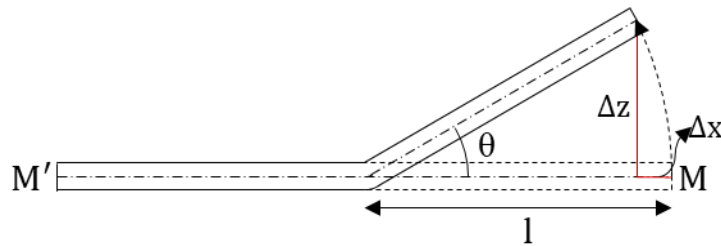


Fig. 3. **MM'** cross-sectional view (cross-sectional cut of the part with a plan with a normal vector along the y direction)

Hence, if the sheet is subjected to θ bending angle, Δx , and Δz can be driven as a function of θ and, l_1 as following:

$$\Delta x = l_1 (1 - \cos \theta) \tag{1}$$

$$\Delta z = l_1 \sin \theta \tag{2}$$

Due to the inherent dependence between Δx and Δz parameters, any attempt to modify one inherently involves an adjustment in the other parameter in this forming strategy. In order to be more accurate, calculation of the forming tool size effect is necessary. The roundness of the forming roller edge (r) results in the float contact point with the workpiece on the forming roller. The contact point is a function of the θ and roundness radius r , see Fig. 4. By applying the Δx , and Δz the contact point in xz plane shifts from P_1 to P_2 as a result of the forming roller size effect.

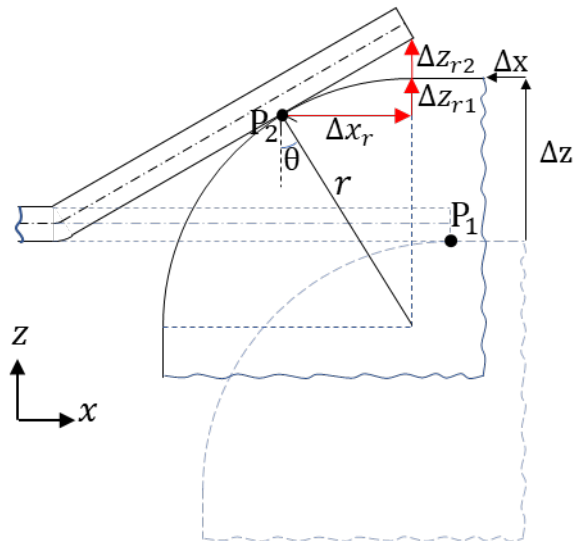


Fig. 4. Schematic of the effect of the r on forming roller-sheet contact

In Fig. 4 red arrows show the movement is needed to eliminate the effect of forming roller edge roundness. Difference between the on-work contact (P_2) point and the initial contact point (P_1) along x direction can be calculated as follows:

$$\Delta x_r = r \sin \theta \tag{3}$$

and along z -direction:

$$\Delta z_{r1} = r(1 - \cos \theta) \tag{4}$$

$$\Delta z_{r2} = \frac{r(1 - \cos \theta)}{\cos \theta} \tag{5}$$

Therefore, Δz_r is equal to:

$$\Delta z_r = \Delta z_{r1} + \Delta z_{r2} = \frac{r \sin^2 \theta}{\cos \theta} \tag{6}$$

Similarly, the radius of the forming roller (R) can result in the float contact point with the workpiece on the forming roller. The float contact point position is a function of R and φ . By applying the Δz is needed to create the θ angle, the contact point in yz plane, shifts from Q_1 to Q_2 as a result of the forming roller size effect, see Fig. 5.

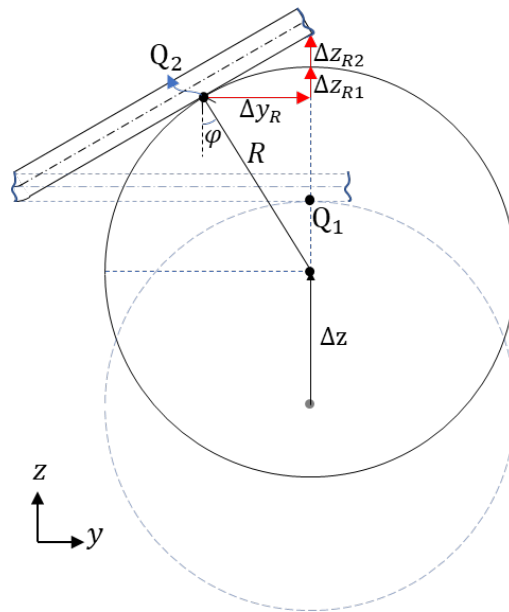


Fig. 5. Schematic of the effect of the R on forming roller-sheet contact

Therefore, the difference between the on-work contact point and the initial contact point along y direction can be calculated as following:

$$\Delta y_R = R \sin \varphi \tag{7}$$

and along z -direction:

$$\Delta z_{R1} = R(1 - \cos \varphi) \tag{8}$$

$$\Delta z_{R2} = \frac{R(1 - \cos \varphi)}{\cos \varphi} \tag{9}$$

Therefore, Δz_R is equal to:

$$\Delta z_R = \frac{R \sin^2 \varphi}{\cos \varphi} \tag{10}$$

Therefore, if the initial position of the forming roller is assumed to be $P_0(x_0, y_0, z_0)$ and its desired final position is assumed to be $P_{f_ideal}(x_{f_ideal}, y_{f_ideal}, z_{f_ideal})$. Therefore:

$$\Delta P_{ideal} = P_{f_ideal} - P_0 \tag{11}$$

$$\Delta x_{ideal} = x_{f_ideal} - x_0 \tag{12}$$

$$\Delta y_{ideal} = y_{f_ideal} - y_0 \tag{13}$$

$$\Delta z_{ideal} = z_{f_ideal} - z_0 \tag{14}$$

Therefore, the final real position of the forming roller considering the r and R effect can be calculated as following:

$$x_{f_real} = x_0 + \Delta x_{ideal} + \Delta x_r \tag{15}$$

$$y_{f_real} = y_0 + \Delta y_{ideal} + \Delta y_R \tag{16}$$

$$z_{f_real} = z_0 + \Delta z_{ideal} + \Delta z_r + \Delta z_R \tag{17}$$

Tool path

For tool path calculation R and r as the constants of the forming roller and l, L, and θ as the parameters related to the geometry of the workpiece is needed which are provided in Table 1.

Table 1: Geometrical parameters of the forming roller and workpiece for tool path generation

R (mm)	r (mm)	l (mm)	L (mm)	θ range
175	5	50	500	0°-60°

The workpiece mentioned in the “part” section has been manufactured and numerically simulated using two different toolpaths following the above-mentioned toolpath theory. I) Part A: using a linear toolpath II) Part B: using a combination of two linear toolpaths

Numerical Simulation

To evaluate the tool path effect on the final geometry and reach an in-depth knowledge of the process, experiments were simulated in the LS-DYNA™ software environment and solved by the explicit solver. A 0.8 mm thick steel strip with a length of 500 mm and width of 100 mm was modeled as a deformable body and a 175 mm dia. forming roller with a width of 35 mm and edge roundness of 5 mm was modeled as a rigid body. Both the strip and forming roller were meshed by fully integrated shell elements with a 1 mm average mesh size and 5 integration points along the thickness. The stripe was modeled based on the results of the tensile tests results which were reported in the material section, using the Hollomon work hardening model. The dynamic friction coefficient of 0.2 was considered between the forming roller and the stripe. The tool paths were applied based on the formula introduced in the toolpath theory section.

Results and discussion

Fig. 6 a and b shows the photograph of the part A and B, respectively. It is evident that while part A was manufactured without any wrinkling defects, a wrinkling defect was observed in the vicinity of $y = 350$ mm in part B. To obtain a thorough comprehension of the wrinkling defect, the parts were scanned using a 7-axis CMM Nikon MCAx 3D laser scanner with a precision of ± 0.01 mm.

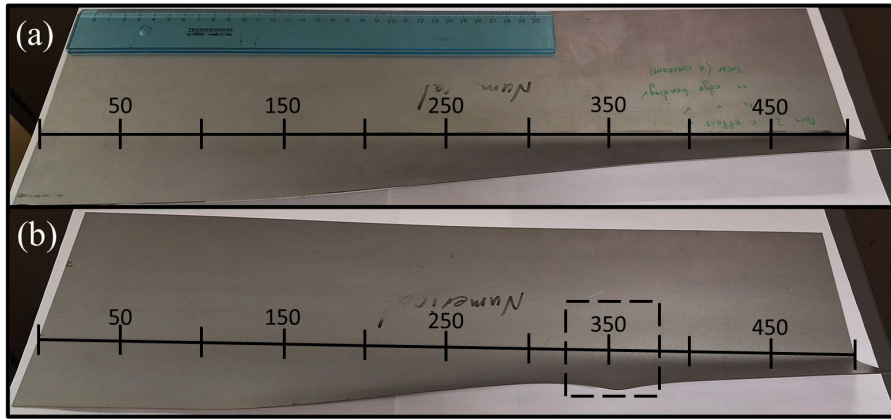


Fig. 6. The workpiece photograph for (a) part A; (b) part B

The intersection of parts A and B with eleven parallel planes, each at a constant distance of 50 millimeters and with a normal vector along the y-direction, is presented in Fig 7 a and b. On the other hand, the cross sectional view of the ideal target part is presented in Fig 7 (c)

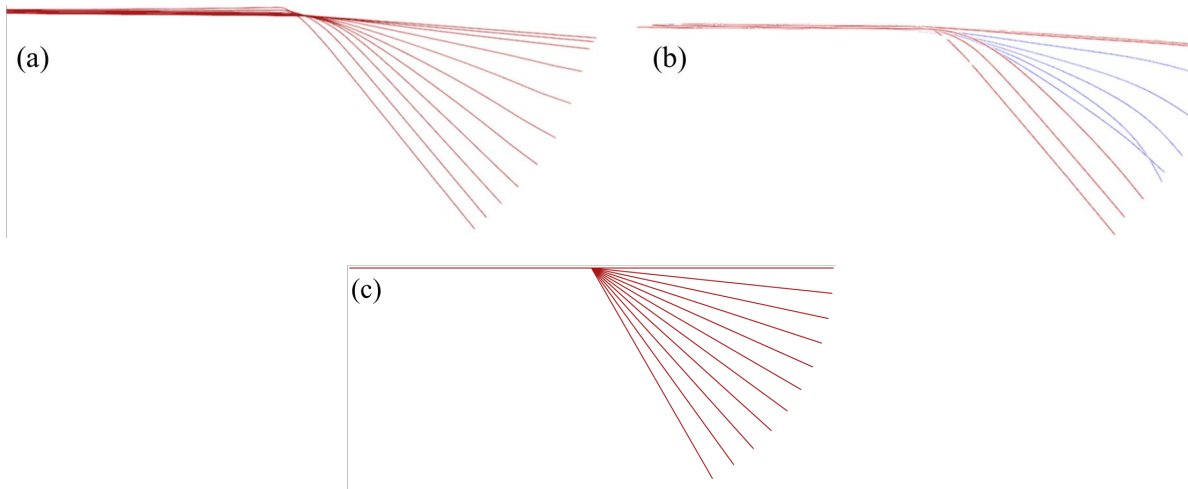


Fig. 7. cross sectional view of the (a) part A; (b) part B (c) ideal target part

In the case of part A, cross sectional cuts revealing the straight flange, except the vicinity of the AA' line in all cross sections. However, in the case of part B, curved flange observed in the cross sections captured in the range of $y = 150$ mm to $y = 350$ mm which indicated with blue color in Fig. 7b. The curved flange leads to change the stripe-roller contact point from the round edge to lateral side of the forming roller. In part B, where a two-stage toolpath has been employed in its manufacturing, the tool gets very close to the edge of the sheet in the vicinity of the $y = 250$ mm and slipping of the sheet on the roller edge and following lateral contact situation which results in wrinkling in vicinity of $y = 350$ mm. Results of 3d scanning demonstrate that flange angle varies from 4° to 50° and from 3° to 50° for part A and B, respectively. As it mentioned above, flange angle varies from 0° to 60° in the ideal target part.

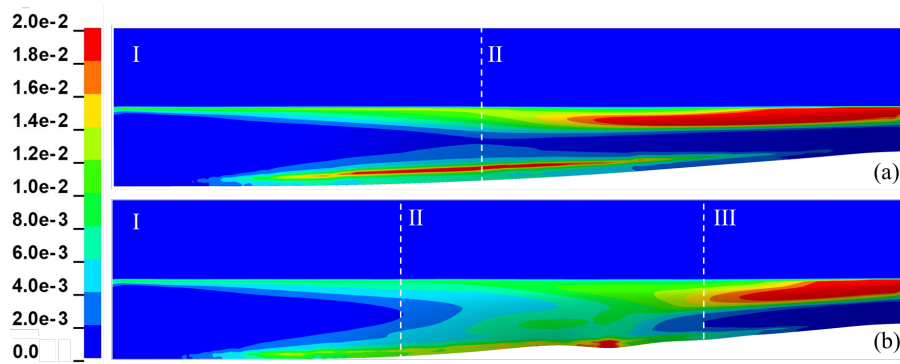


Fig. 8. Effective plastic strain of (a) part A; (b) part B

Fig. 8 a and b show the results of the numerical simulation of the process for part A and B respectively. Bent angle measurement of cross-sectional cuts shows that flange angle varies in the 5° - 55° and 5° - 54° range for part A and B, respectively. In the case of Part B, wrinkling occurs in $y = 345$ mm, while part A manufactured without wrinkling effect. For a more detailed review, the part A can be divided into two sections: I) Both deformation area and strain intensity are ascending with respect to y amount. II) In this section, the deformation area is descending, and strain intensity is ascending with respect to y amount. Near the border of the section I and II secondary deformation has been observed in the contact point of the stripe-forming roller. On the other hand, part B can be divided into three sections: I) Both deformation area and strain intensity are ascending with respect to y amount, same with part A. II) in this section, plastic deformation occurs throughout the entire flange, leading to the curved flange and wrinkling defect. III) In this section, the deformation area is descending and strain intensity is ascending with respect to y amount, same with part A. section II of part A and section III of part B is ideal. Because the deformation area is concentrated and secondary deformation is negligible.

Conclusions

The paper presented the theory of the tool path for incremental roll profiling. Number of the increments has a profound impact on the geometrical accuracy of the manufactured part. As the number of increments increases, the tool approaches the edge of the sheet, heightening the probability of stripe contact with the lateral surface of the roller which results in curved flange profile and wrinkling defect. Therefore, it's recommended to increase the roller-stripe contact point distance from the flange edge in the case of the increasing of the number of the increments. Presented results shows the capability of the introduced incremental forming process in manufacturing of the complex geometries.

Acknowledgments

This study was carried out within the PNRR research activities of the consortium iNEST (Interconnected North-Est Innovation Ecosystem) funded by the European Union Next-GenerationEU (Piano Nazionale di Ripresa e Resilienza (PNRR) – Missione 4 Componente 2, Investimento 1.5 – D.D. 1058 23/06/2022, ECS_00000043). This manuscript reflects only the Authors' views and opinions, neither the European Union nor the European Commission can be considered responsible for them.

References

- [1] Monostori, László, Botond Kádár, Thomas Bauernhansl, Shinsuke Kondoh, Soundar Kumara, Gunther Reinhart, Olaf Sauer, Gunther Schuh, Wilfried Sihn, and Kenichi Ueda, *Cyber-physical systems in manufacturing*, *Cirp Annals* 65, no. 2 (2016): 621-641. <https://doi.org/10.1016/j.cirp.2016.06.005>

- [2] Kazancoglu, Ipek, Melisa Ozbiltekin-Pala, Sachin Kumar Mangla, Yigit Kazancoglu, and Fauzia Jabeen, Role of flexibility, agility and responsiveness for sustainable supply chain resilience during COVID-19, *Journal of Cleaner Production* 362 (2022): 132431. <https://doi.org/10.1016/j.jclepro.2022.132431>
- [3] Ambrogio, G., Luigino Filice, and F. Gagliardi, Formability of lightweight alloys by hot incremental sheet forming, *Materials & Design* 34 (2012): 501-508. <https://doi.org/10.1016/j.matdes.2011.08.024>
- [4] Dang, Xiaobing, Kai He, Feifei Zhang, Qiyang Zuo, and Ruxu Du, Multi-stage incremental bending to form doubly curved metal plates based on bending limit diagram, *International Journal of Mechanical Sciences* 155 (2019): 19-30. <https://doi.org/10.1016/j.ijmecsci.2019.02.001>
- [5] Ambrogio, G., L. De Napoli, L. Filice, F. Gagliardi, and M. Muzzupappa, Application of Incremental Forming process for high customised medical product manufacturing, *Journal of materials processing technology* 162 (2005): 156-162. <https://doi.org/10.1016/j.jmatprotec.2005.02.148>
- [6] Attanasio, Aldo, Elisabetta Ceretti, Claudio Giardini, and Luca Mazzoni, Asymmetric two points incremental forming: improving surface quality and geometric accuracy by tool path optimization, *Journal of materials processing technology* 197, no. 1-3 (2008): 59-67. <https://doi.org/10.1016/j.jmatprotec.2007.05.053>
- [7] Deole, Aditya D., Matthew R. Barnett, and Matthias Weiss, The numerical prediction of ductile fracture of martensitic steel in roll forming, *International Journal of Solids and Structures* 144 (2018): 20-31. <https://doi.org/10.1016/j.ijsolstr.2018.04.011>
- [8] Kim, Dongun, MyungHwan Cha, and Yeon Sik Kang, Development of the bus frame by flexible roll forming, *Procedia Engineering* 183 (2017): 11-16. <https://doi.org/10.1016/j.proeng.2017.04.004>
- [9] Abeyrathna, Buddhika, Bernard Rolfe, Libo Pan, Rui Ge, and Matthias Weiss, Flexible roll forming of an automotive component with variable depth, *Advances in Materials and Processing Technologies* 2, no. 4 (2016): 527-538. <https://doi.org/10.1080/2374068X.2016.1247234>
- [10] Groche, Peter, Arnd Zettler, Sebastian Berner, and Georg Schneider, Development and verification of a one-step-model for the design of flexible roll formed parts, *International journal of material forming* 4 (2011): 371-377. <https://doi.org/10.1007/s12289-010-0998-3>
- [11] Jeswiet, J., F. Micari, G. Hirt, A. Bramley, Joost Dufloy, and J. Allwood, Asymmetric single point incremental forming of sheet metal, *CIRP annals* 54, no. 2 (2005): 88-114. [https://doi.org/10.1016/S0007-8506\(07\)60021-3](https://doi.org/10.1016/S0007-8506(07)60021-3)
- [12] Patel, Dharmin, and Anishkumar Gandhi, A review article on process parameters affecting Incremental Sheet Forming (ISF), *Materials Today: Proceedings* 63 (2022): 368-375. <https://doi.org/10.1016/j.matpr.2022.03.208>
- [13] Jackson, Kathryn, and Julian Allwood, The mechanics of incremental sheet forming, *Journal of materials processing technology* 209, no. 3 (2009): 1158-1174. <https://doi.org/10.1016/j.jmatprotec.2008.03.025>
- [14] Music, O., J. M. Allwood, and K. Kawai, A review of the mechanics of metal spinning, *Journal of materials processing technology* 210, no. 1 (2010): 3-23. <https://doi.org/10.1016/j.jmatprotec.2009.08.021>

- [15] Russo, Iacopo M., Christopher J. Cleaver, and Julian M. Allwood, Seven principles of toolpath design in conventional metal spinning, *Journal of Materials Processing Technology* 294 (2021): 117131. <https://doi.org/10.1016/j.jmatprotec.2021.117131>
- [16] Voswinckel, Holger, Markus Bambach, and Gerhard Hirt, Process limits of stretch and shrink flanging by incremental sheet metal forming, *Key engineering materials* 549 (2013): 45-52. <https://doi.org/10.4028/www.scientific.net/KEM.549.45>
- [17] Voswinckel, Holger, Markus Bambach, and Gerhard Hirt, Improving geometrical accuracy for flanging by incremental sheet metal forming, *International Journal of Material Forming* 8 (2015): 391-399. <https://doi.org/10.1007/s12289-014-1182-y>
- [18] Buranathiti, Thaweeapat, Jian Cao, Wei Chen, Lusine Baghdasaryan, and Z. Cedric Xia, Approaches for model validation: methodology and illustration on a sheet metal flanging process, *J. Manuf. Sci. Eng.* 128, no. 2 (2006): 588-597. <https://doi.org/10.1115/1.1807852>
- [19] Le Maoût, Nicolas, S. Thuillier, and P. Y. Manach, Classical and roll-hemming processes of pre-strained metallic sheets, *Experimental mechanics* 50 (2010): 1087-1097. <https://doi.org/10.1007/s11340-009-9297-7>
- [20] Wang, Jian Qiang, Ya Wen Huang, Guang Rui Zhou, Zhao Long Niu, and Zi Wen Cheng, Process Parameters Study on Robot Rope Hemming of the Hood, *Applied Mechanics and Materials* 602 (2014): 950-953. <https://doi.org/10.4028/www.scientific.net/AMM.602-605.950>
- [21] Hu, Xing, Yi Xi Zhao, Shu Hui Li, and Cheng Liu, Numerical Simulation of Dimensional Variations for Roller Hemming, *Advanced Materials Research* 160 (2011): 1601-1605. <https://doi.org/10.4028/www.scientific.net/AMR.160-162.1601>
- [22] Simonetto, Enrico, Andrea Ghiotti, Stefania Bruschi, and Stefano Filippi, Flexible Incremental Roller Flanging process for metal sheets profiles, *Procedia CIRP* 103 (2021): 219-224. <https://doi.org/10.1016/j.procir.2021.10.035>
- [23] Simonetto, Enrico, Andrea Ghiotti, and Stefania Bruschi, Agile manufacturing of complex shaped bent profiles by incremental deformation, *Manufacturing Letters* 36 (2023): 40-43. <https://doi.org/10.1016/j.mfglet.2023.01.004>